Report no. 07/15

New quadrature formulas from conformal maps

by
Nicholas Hale
Lloyd N. Trefethen

Gauss and Clenshaw–Curtis quadrature, like Legendre and Chebyshev spectral methods, make use of grids strongly clustered at boundaries. From the viewpoint of polynomial approximation this seems necessary and indeed in certain respects optimal. Nevertheless such methods may "waste" a factor of $\pi/2$ with respect to each space dimension. We propose new non-polynomial quadrature methods that avoid this effect by conformally mapping the usual ellipse of convergence to an infinite strip or another approximately straight-sided domain. The new methods are compared with related ideas of Bakhvalov, Kosloff and Tal-Ezer, Rokhlin and Alpert, and others. An advantage of the conformal mapping approach is that it leads to theorems guaranteeing geometric rates of convergence for analytic integrands. For example, one of the formulas presented is proved to converge 50% faster than Gauss quadrature for functions analytic in an ε-neighborhood of $[-1, 1]$.

Oxford University Computing Laboratory
Numerical Analysis Group
Wolfson Building
Parks Road
Oxford, England OX1 3QD

June, 2007

1 Introduction

The Gauss and Clenshaw–Curtis quadrature formulas, as well as other related numerical methods for integration of nonperiodic functions or spectral solution of nonperiodic ODEs or PDEs, all cluster the gridpoints near the boundaries. Indeed, for any convergent numerical method derived from polynomial interpolation in the grid points, the clustering will be asymptotically the same: on $[-1,1]$, n points will be distributed with density $\sim n/(\pi\sqrt{1-x^2})$ as $n \to \infty$ [36, Thm. 12.7].

It is well known that this clustering may cause problems. The high density of points near the boundaries may necessitate very small time steps in an explicit time-stepping spectral method, or make the matrices involved in implicit time-stepping terribly ill-conditioned [12, 49]. At the same time the low density of points in the middle of the domain may force one to use more points than "ought" to be needed to resolve the solution. Compared with equally-spaced grids, these clustered grids have $\pi/2$ times coarser spacing in the middle, implying that for many calculations, n must be about $\pi/2$ times larger than one might expect. In a three-dimensional calculation, a discretization may need $(\pi/2)^3 \approx 4$ times as many grid points as one would like. Such a factor may have a large impact on the cost of linear algebra operations.

In this article we focus on this $\pi/2$ problem and mainly on quadrature, not spectral methods. The problem arises in purest form if we consider the integral from -1 to 1 of a function f analytic in a narrow strip about the real axis. If f is periodic, we can use the trapezoid rule and get geometric convergence. If f is not periodic, the trapezoid rule loses its speed, but Gauss quadrature still converges geometrically. However, the rate is $\pi/2$ times slower.

Various authors have proposed methods for countering this effect. We shall suggest a new approach based on conformal mapping, which leads to formulas that converge more quickly than Gauss quadrature for many integrands. The practical performance of our methods is not much different from that of other methods in the literature, such as those of Alpert [3] and Kosloff and Tal-Ezer [33] (see §5). Nevertheless, the conformal mapping idea has advantages. First, it is conceptually clear, simple, and flexible, explaining in a precise way the nature of the $\pi/2$ effect and exactly what improvements may be possible for integrands analytic in specified domains. Second, it leads immediately to theorems on geometric convergence rates for analytic integrands. In the existing literature of related methods, it is hard to find such theorems. An additional advantage, which we shall not discuss further, is that the conformal mapping approach connects these simple quadrature problems to more complicated problems where conformal maps have also proved useful, such as the Double Exponential quadrature formula and Tee's adaptive rational spectral methods [47, 48].

An outline of the article is as follows. In §2 we present the conformal transplantation idea. We apply it in §3 to the particular case of a map to an infinite strip and in §4 to a simpler variant that may be equally useful in practice. Related work is surveyed in §5, and theorems about geometric convergence rates are presented in §6. The Clenshaw–Curtis variant of our formulas is considered in §7, and we close in §8 with a summary discussion. The Appendix includes a 14-line FFT-based MATLAB code that runs in

less than a second for n as high as 10^5 yet usually delivers more accurate integrals than the Gauss rule for each value of n.

2 Transplanted quadrature formulas

Let f be an analytic function on $[-1,1]$ whose integral

$$I = I(f) = \int_{-1}^{1} f(x)dx \tag{2.1}$$

we seek to calculate. A general interval $[a,b]$ can be handled by a linear change of variables. All the methods we shall consider approximate I by sums

$$I_n = I_n(f) = \sum_{k=1}^{n} w_k f(x_k) \tag{2.2}$$

defined by *nodes* $\{x_k\}$ and *weights* $\{w_k\}$. *Polynomial methods* of this kind are based on the following principle: given nodes $\{x_k\}$, the weights $\{w_k\}$ are chosen so that I_n is equal to the integral of the unique degree $n-1$ polynomial interpolant through the data points. In particular, Newton–Cotes quadrature is obtained from equally spaced nodes, Gauss quadrature from the roots of the Legendre polynomial P_n, and Clenshaw–Curtis quadrature from the Chebyshev points $x_k = \cos((k-1)\pi/(n-1))$. Any polynomial method that converges as $n \to \infty$ for all analytic f must have its nodes distributed asymptotically with density $\sim n/(\pi\sqrt{1-x^2})$ as $n \to \infty$. The Gauss and Clenshaw–Curtis formulas have this property, and converge for any continuous f. The Newton–Cotes formulas do not, and diverge in general even if f is analytic [5, 36, 41].

The standard theorems about convergence of polynomial methods for analytic functions assume that the integrand is analytic in an elliptical region. For any $\rho > 1$, let us define E_ρ to be the open set in the complex plane bounded by the ellipse with foci ± 1 with semiminor and semimajor axis lengths summing to ρ. This ellipse can also be described as the image of the circle of radius ρ about the origin under the map $w = (z + z^{-1})/2$. The general idea of the following convergence theorem goes back to Bernstein in 1919 [8], but such results do not appear in many textbooks or monographs and there is not much uniformity in the constants that one finds on the right-hand side [25, p. 114]. The particular result presented here is due to Rabinowitz [42, eq. (18)]; see also [11, Thm. 90] and [50, Thm. 4.5].

Theorem 1 *If f is analytic in E_ρ with $|f(z)| \le M$ for some $\rho > 1$, then Gauss quadrature converges geometrically with the bound*

$$|I_n - I| \le \frac{64M}{15(1-\rho^{-2})\rho^{2n}} \qquad (n \ge 0). \tag{2.3}$$

When we don't care about constants, we may simply note that Theorem 1 ensures geometric convergence at the rate $O(\rho^{-2n})$ as $n \to \infty$.

To experts in approximation theory, the assumption of analyticity in an elliptical region is so familiar as to seem almost beyond question. Nevertheless, the appearance of ellipses in this analysis is driven not by the quadrature formula (2.2) per se, but by the decision to derive weights from polynomial interpolation. If we do not insist on polynomials, ellipses cease to have any special status.

We have already observed from the uneven distribution of Gauss and Clenshaw–Curtis nodes that there may be a reason to move beyond polynomials. Here is another argument based on the shape of E_ρ. From an applications point of view, the assumption that f is analytic in E_ρ is unbalanced, for it permits f to be "less analytic" near the ends of the interval, where the ellipse is narrow, than in the middle, where it is wide. Specifically, the Taylor series of f at a point $x \approx \pm 1$ is allowed to have more rapidly increasing coefficients than are permitted at a point $x \approx 0$. This nonuniform analyticity condition leads to Theorem 1 and related results for other polynomial quadrature formulas, but it has no intrinsic justification. Further consequences of the same nonuniformity reverberate throughout the field of polynomial approximation theory—for example, in the book by Ditzian and Totik [17]. Of course, there are applications where the functions of interest do have less smoothness near the boundary than in the interior, such as fluid mechanics problems with boundary layers. Even here, however, there is no reason to expect that an ellipse should be exactly the right region to consider. Weak boundary layers might benefit from less grid clustering at boundaries, and strong ones from even more.

Our plan is to derive new quadrature formulas (2.2) for $[-1,1]$ by conformally mapping E_ρ to a region Ω_ρ that has straighter sides. We describe the procedure first in general terms; see Figure 1.

Let Ω_ρ be an open set in $\mathbb{C}$ containing $[-1,1]$. Let g be an analytic function in E_ρ satisfying

$$g(E_\rho) \subseteq \Omega_\rho, \qquad g(-1) = -1, \quad g(1) = 1. \tag{2.4}$$

Then $g([-1,1])$ is an analytic curve in Ω_ρ, parametrized by $s \in [-1,1]$, that connects -1 to 1. By Cauchy's theorem for analytic functions, the integral of f over this curve is the same as the integral of f over $[-1,1]$ itself. Thus (2.1) can be rewritten

$$I(f) = \int_{-1}^{1} g'(s) f(g(s)) ds. \tag{2.5}$$

If we apply (2.2) to this integral in the s variable, we obtain

$$I_n(\, g' \cdot (f \circ g)) = \sum_{k=1}^{n} w_k g'(x_k) f(g(x_k)),$$

which can be rewritten in the form (2.2) as

$$\boxed{\tilde{I}_n = \tilde{I}_n(f) = \sum_{k=1}^{n} \tilde{w}_k f(\tilde{x}_k), \quad \tilde{w}_k = w_k g'(x_k), \quad \tilde{x}_k = g(x_k).} \tag{2.6}$$

TRANSPLANTED QUADRATURE FORMULA

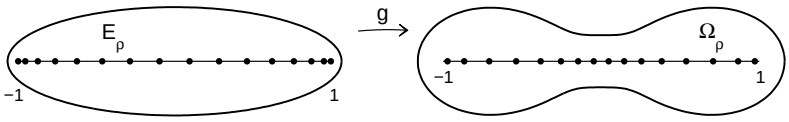

Figure 1: A transplanted quadrature formula (2.6) is defined by an analytic function g that maps the elliptical region E_ρ into a region Ω_ρ containing $[-1,1]$. In this illustration the map is $g(s) = 0.5s + 0.2s^3 + 0.3s^5$ with $\rho = 1.4$. The dots show Gauss points $x_k \in E_\rho$ for $n = 16$ and their images $\tilde{x}_k \in \Omega_\rho$.

In this article we generally speak of g as a conformal map, which is defined as an analytic function with nonvanishing derivative that maps one region bijectively onto another. In fact, for the theorems we present g does not actually have to be conformal, merely analytic. Nor does g have to map $[-1,1]$ into itself; it could take complex values. For the formulas of practical interest, however, these extra conditions will usually be satisfied, and if they are, then we have the additional properties that the nodes $\tilde{x}_k$ are real and the weights $\tilde{w}_k$ are real and positive. In some applications to spectral methods, not considered here, conformality is genuinely required.

The following theorem on convergence of transplanted Gauss quadrature is a corollary of Theorem 1.

Theorem 2 *Let f be analytic in a region Ω_ρ containing $[-1,1]$ with $|f(z)| \le M$ for some $\rho > 1$, and let a transplanted Gauss quadrature formula* (2.6) *be defined by some map g satisfying* (2.4)*. Then*

$$|\tilde{I}_n - I| \le \frac{64M\gamma}{15(1-\rho^{-2})\rho^{2n}} \qquad (n \ge 0),$$

where $\gamma = \sup_{s\in E_\rho} |g'(s)| \le \infty$.

If $\gamma = \infty$ in this estimate, we can shrink ρ a little bit to make it finite. Thus transplanted Gauss quadrature always converges geometrically if f is analytic on $[-1,1]$.

3 Map to an infinite strip

We now turn to particular choices of the map g that may be useful in practice. Since our aim is to make the sides of Ω_ρ straighter than those of E_ρ, we begin by taking this notion as far as possible and considering the map g that takes E_ρ to an infinite strip Ω_ρ symmetric about the real axis with $g(\pm 1) = \pm 1$ and the ends of the ellipse mapping to $\pm\infty$ (Figure 2). These conditions determine g fully. The half-width a of Ω_ρ is not adjustable but is determined by the value of ρ (equation (3.5) below).

The map of the ellipse to the strip can be constructed in three steps (Figure 3). Let F_s denote the upper half of E_ρ, with distinguished boundary points $s_A = 0$, $s_B = 1$, and

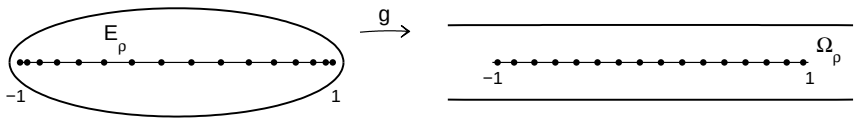

Figure 2: One choice of Ω_ρ is an infinite strip, shown here again for $\rho = 1.4$. The semiminor axis length of E_ρ is $\sim (\rho - 1)$, whereas the half-width of Ω_ρ is $\sim (2/\pi)(\rho - 1)$, reflecting the $\pi/2$ times weaker analyticity requirement of the transplanted quadrature formula. Note how the Gauss nodes in E_ρ map to nodes in Ω_ρ that are so close to equally spaced that they appear almost exactly even. For more on this spacing see Figure 9.

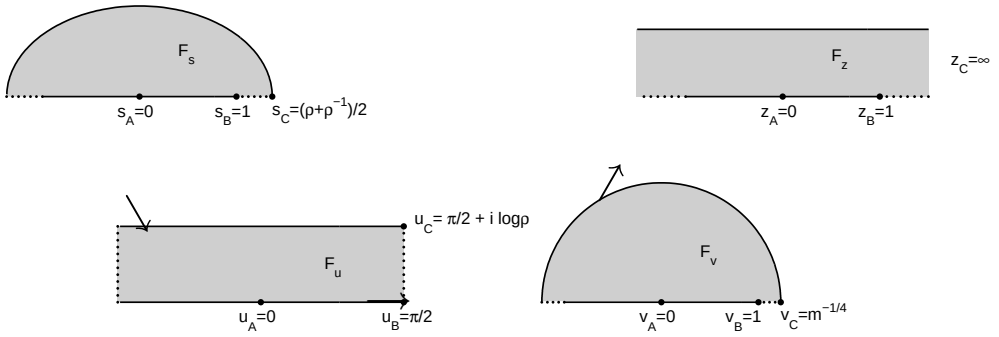

Figure 3: Construction of the strip map in three steps $s \to u \to v \to z$. The upper half of each region is shown. A large value of ρ has been used for clarity ($\rho = 2.3$), since as ρ decreases to 1, the segment from v_B to v_C shrinks exponentially.

$s_C = (\rho + \rho^{-1})/2$ (the right endpoint of E_ρ). The function $u = \sin^{-1} s$ maps F_s to the rectangle F_u of width π and height $\log \rho$ with corresponding boundary points $u_A = 0$, $u_B = \pi/2$, $u_C = \pi/2 + i \log \rho$. We now map F_u to a half-disk by a Jacobi elliptic sine function sn with parameter m [1, 20]. Specifically, $v = \mathrm{sn}(2Ku/\pi \,|\, m)$ maps F_u to the upper half-disk F_v about the origin of radius $m^{-1/4}$, with $v_A = 0$, $v_B = 1$, $v_C = m^{-1/4}$. Here, following standard notation, the parameter m with $0 < m < 1$ is chosen such that the associated elliptic integrals K' and K satisfy $K'/K = 4 \log(\rho)/\pi$. Given ρ, the appropriate value of m can be calculated by the rapidly convergent series expression given in [24],

$$m^{1/4} = 2 \sum_{j=1}^{\infty} \rho^{-4(j-\frac{1}{2})^2} \Big/ \left(1 + 2 \sum_{j=1}^{\infty} \rho^{-4j^2}\right). \tag{3.1}$$

Finally $z = \tanh^{-1}(m^{1/4} v) / \tanh^{-1}(m^{1/4})$ maps F_v to F_z, the upper half of an infinite strip about the real axis with $z_A = 0$, $z_B = 1$, $z_C = +\infty$. Combining the steps, we have the ellipse $\to$ strip map

$$g(s) = \tanh^{-1}\left(m^{1/4} \,\mathrm{sn}\left(\frac{2K}{\pi} \sin^{-1}(s) \,|\, m\right)\right) \Big/ \tanh^{-1}(m^{1/4}) \,. \tag{3.2}$$

The same formula is valid also below the real axis (by the Schwarz reflection principle),

and thus g as given by (3.2) maps all of E_ρ to all of Ω_ρ. For the transplanted quadrature formula (2.6) we also require the derivative of the map function, which for $s \in (-1,1)$ is given by

$$g'(s) = \frac{2Km^{1/4}}{\pi\sqrt{1-s^2}} \frac{\mathrm{cn}(\omega|m)\,\mathrm{dn}(\omega|m)}{(1-m^{1/2}\mathrm{sn}^2(\omega|m))} \Big/ \tanh^{-1}(m^{1/4}) \tag{3.3}$$

where $\omega = 2K\sin^{-1}(s)/\pi$. For the endpoints $s = \pm 1$, with the aid of L'Hopital's rule one can derive the formula

$$g'(\pm 1) = 4K^2\pi^{-2}m^{1/4}(1+m^{1/2}), \tag{3.4}$$

which we shall need for the Clenshaw–Curtis variant in §7.

The half-width a of Ω_ρ is

$$a = \frac{\pi}{4\tanh^{-1}(m^{1/4})} < \frac{2}{\pi}(\rho-1), \tag{3.5}$$

with $a \sim (2/\pi)(\rho-1)$ as $\rho \to 1$ (we have verified this inequality numerically, and no doubt it could be proved analytically). The half-width of E_ρ in the same limit is $\sim(\rho-1)$. Thus the transplanted formula needs only $2/\pi$ times as wide a strip of analyticity to achieve the same convergence rate, as is confirmed by the following theorem. Further convergence results for this method are given in §6.

Theorem 3 *Let f be analytic in the strip Ω_ρ about $\mathbb{R}$ of half-width $(2/\pi)(\rho-1)$ for some $\rho > 1$. Let f be integrated by the transplanted Gauss quadrature formula* (2.6) *associated with the map* (3.2) *from E_ρ to Ω_ρ. Then for any $\tilde\rho < \rho$,*

$$\tilde I_n - I = O(\tilde\rho^{-2n}) \qquad (n \to \infty). \tag{3.6}$$

Proof The inequality (3.5) implies that $f(x)$ is analytic in the strip of half-width a, and therefore $f(g(s))$ is analytic in E_ρ. The constant γ of Theorem 2 is infinite for this map g, so we do not quite get $O(\rho^{-2n})$ convergence, and for this reason we have not assumed that f is bounded either. For any $\tilde\rho < \rho$, however, Theorem 1 still applies to the integrand $g'(s)f(g(s))$ of (2.5), which will be analytic and bounded in this smaller ellipse. This implies (3.6). ∎

To make our domain narrower in the imaginary direction by a factor of $2/\pi$, we have lengthened it in the real direction by a factor of ∞! This may seem a dubious improvement, and indeed, it is a very strong condition that f must be analytic throughout an infinite strip. However, this is not a serious issue in practice because if we consider slightly smaller $\tilde\rho$-ellipses within E_ρ, we find that they map under g to domains about $[-1,1]$ that are much shorter. Thus little is lost if f is analytic near $[-1,1]$ but not very far down the real axis. Figure 4 illustrates this effect.

Let us see how strip-transplanted Gauss quadrature performs in practice. We do not normally recommend tuning ρ to the integrand at hand, for we are hardly likely to beat adaptive quadrature methods at their own game. Instead the aim is to derive a fixed

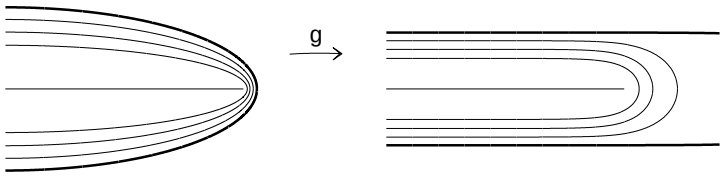

Figure 4: Though g maps E_ρ to the unbounded strip Ω_ρ, it maps smaller ellipses within E_ρ to regions that hug the interval $[-1,1]$ closely. Because of this property, f does not have to be analytic far down the strip for transplanted Gauss quadrature to be effective. Also, since the subregions have nearly straight sides, a value of ρ chosen for the strip of a particular half-width will also be effective for integrands whose true regions of analyticity are narrower.

family of formulas that perform well, if not quite optimally, and with this in mind we start by fixing the value $\rho = 1.4$ arbitrarily, as in Figures 1–2. Figure 5 shows that for many integrands, the result is a clear improvement over Gauss quadrature. (For this relatively large value of ρ, the improvement factor is about 1.42 rather than $\pi/2 \approx 1.57$.) This occurs for example for the first three integrands, which have poles or branch points close to $[-1,1]$ in the complex plane. A similar speedup is observed for the fourth function, $\exp(-40x^2)$, which has no singularities but grows very rapidly as x moves away from the real axis. For the fifth function, $\cos(40x)$, the transplanted quadrature formula begins to converge sooner than the untransplanted one since it resolves the oscillations sooner; once the error falls below 10^{-5}, the untransplanted formula overtakes it because the function is entire. The sixth integrand, $\exp(-x^{-2})$, is C^∞ but not analytic; here we see comparable performance of the two methods. The same is observed for $|x| - |x - 0.1|$, which is continuous but not differentiable. For the eighth integrand, $\sqrt{1.01 - x}$, the untransplanted Gauss rule wins because of its weaker analyticity requirement near ± 1. Finally, for the entire function $\cos(x)$, the transplanted rule loses by a substantial factor because it is stuck at the particular convergence rate $O(\rho^{-2n})$ with $\rho = 1.4$ since g is singular at the endpoints of this ellipse. The standard Gauss formula, by contrast, is not tied to any particular ellipse of analyticity, and thus does very well in a case like this where the integrand is analytic and not too large in a sizable region around $[-1,1]$.

In fact, the convergence rate for the transplanted Gauss formula applied to $\cos(x)$ in Figure 5 has rather little to do with $\cos(x)$—the rate would be almost exactly the same for the integrand $f(x) = 1$! In general, non-polynomial quadrature formulas do not integrate constants exactly.

To implement the transplanted formula (2.6), we need to be able to compute g and g'. The following MATLAB code segment does this for the strip map (3.2). The standard MATLAB functions `ellipke` and `ellipj` used here to compute Jacobi elliptic functions are restricted to real arguments; for the complex values needed in Figures 2 and 4, we replaced `ellipj` by the function `ellipjc` from Driscoll's Schwarz–Christoffel Toolbox [19]. The function `gauss`, from [49], computes Gauss quadrature nodes and weights.

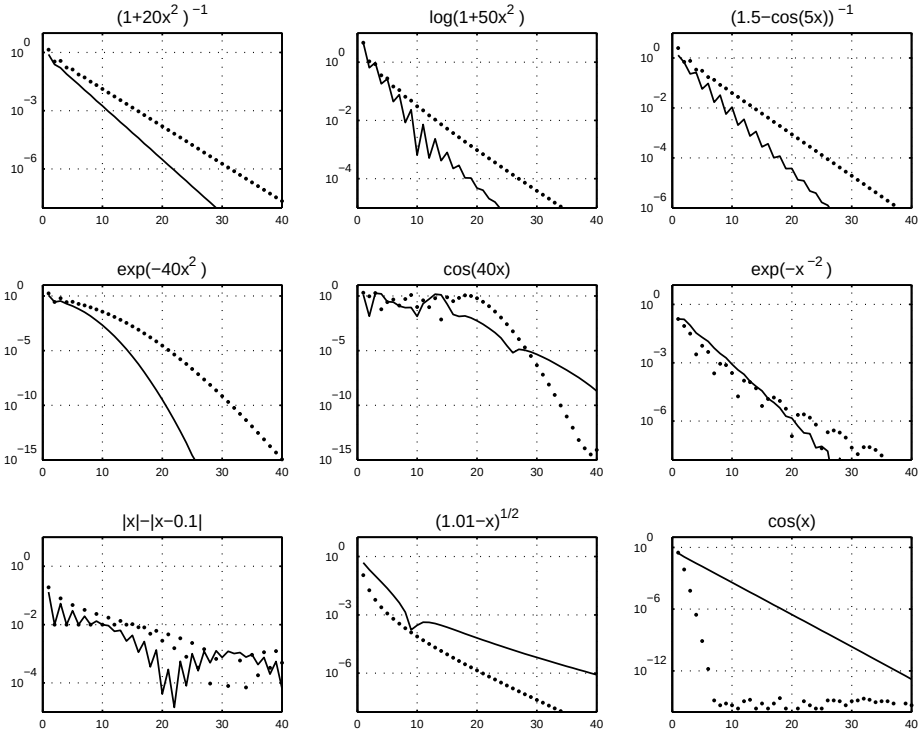

Figure 5: Comparison of Gauss quadrature (dots) against Gauss quadrature transplanted to an infinite strip (solid) for nine integrands on $[-1, 1]$, with $\rho = 1.4$. In a number of cases the transplanted formulas converge about 1.4 times faster.

```
f = @(x) 1./(1+20*x.^2);                % change this for other integrands
[s,w] = gauss(n);                       % Gauss nodes and weights
[g,gprime] = strip(s);                  % g and g'
In = (w.*gprime')*f(g);                 % the integral

function [g,gprime] = strip(s)          % change this for a different map g
rho = 1.4;                              % this can be adjusted
num = 0; den = 0;
for j = 1:round(.5+sqrt(10/log(rho)))   % given rho, find m
  num = num + rho^(-4*(j-.5)^2);
  den = den + rho^(-4*j^2);
end
m4 = 2*num/(1+2*den); m = m4^4;         % m^{1/4} and m
K = ellipke(m);                         % Jacobi elliptic parameter
u = asin(s);
[sn,cn,dn] = ellipj(2*K*u/pi,m);        % Jacobi eliptic function
duds = 1./sqrt(1-s.^2);
dvdu = (2*K/pi)*cn.*dn;
dgdv = (m4./(1-m4.^2*sn.^2))/atanh(m4);
g = atanh(m4*sn)/atanh(m4);             % g
gprime = dgdv.*dvdu.*duds;              % g'
```

If ρ is close to 1 (smaller than about 1.1), the code just given suffers from numerical instability. The Appendix outlines what can be done in such cases, and in fact, it offers a map very slightly different from (3.2) that as a practical matter may be superior.

4 A simpler conformal map

We now put aside the infinite strip and consider another idea for selecting the function g. Suppose we set out to cancel the clustering of Gauss or Clenshaw–Curtis points exactly. The function $g(s) = (2/\pi)\sin^{-1}(s)$ would achieve this, and the factor $2/\pi$ makes it plain that the result would be a grid denser by that factor in the middle of the interval. This choice of g would be useless, however, because $\sin^{-1}(s)$ has singularities at ± 1, so we would have no ellipse of analyticity at all for the transplanted integrand.

Instead we propose taking the terms through degree d of the Taylor series

$$\sin^{-1} s = s + \frac{1}{6}s^3 + \frac{3}{40}s^5 + \frac{5}{112}s^7 + \frac{35}{1152}s^9 + \cdots,$$

and then normalizing so that $g(\pm 1) = \pm 1$ as required by (2.4). Taking $d = 1$, 5, or 9 gives the following choices, respectively:

$$g(s) = s, \tag{4.1}$$

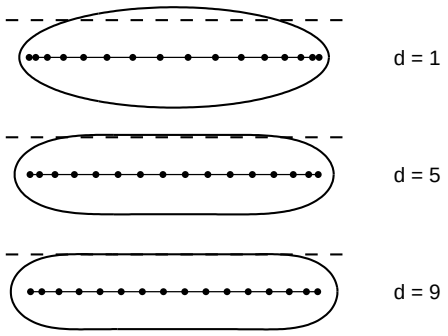

Figure 6: "Sausages" Ω_ρ corresponding to the maps (4.1), (4.2), (4.3) with $\rho = 1.4$. The dashed line in each image marks the target height $(2/\pi)(\rho - 1)$.

$$g(s) = \frac{1}{149}(120s + 20s^3 + 9s^5), \tag{4.2}$$

$$g(s) = \frac{1}{53089}(40320s + 6720s^3 + 3024s^5 + 1800s^7 + 1225s^9). \tag{4.3}$$

Figure 6 shows the corresponding "sausage domains" Ω_ρ for $\rho = 1.4$.[1]

To implement transplanted Gauss quadrature of degree d (odd), we can replace the function `strip` in the code above by the following function `sausage`. The line with the `cumprod` command computes the Taylor series coefficients of $\sin^{-1}(x)$.

```
function [g,gprime] = sausage(s)
d = 9;                                          % this can be adjusted
c = zeros(1,d+1);
c(d:-2:1) = [1 cumprod(1:2:d-2)./cumprod(2:2:d-1)]./(1:2:d);
c = c/sum(c); g = polyval(c,s);
cp = c(1:d).*(d:-1:1); gprime = polyval(cp,s);
```

Figure 7 shows the performance of this method with $d = 9$ for various integrands. On the whole the convergence is much like that with the strip map, though somewhat slower for the first few examples and faster for the last few. With $f(x) = \cos x$, for example, we do much better now since g has no singularity to limit the convergence rate. Although it is entire, however, g still grows rapidly away from $[-1, 1]$, and that is why this map still does not match untransplanted Gauss quadrature for $\cos(x)$.

In §6 we give a theorem that establishes that Gauss quadrature transplanted by (4.3) is 30% faster than standard Gauss quadrature for functions analytic in an ε-neighborhood of $[-1, 1]$.

[1]Previous authors have investigated the conformal mapping of a "bratwurst," but their maps concern exteriors rather than interiors and the applications are different [32].

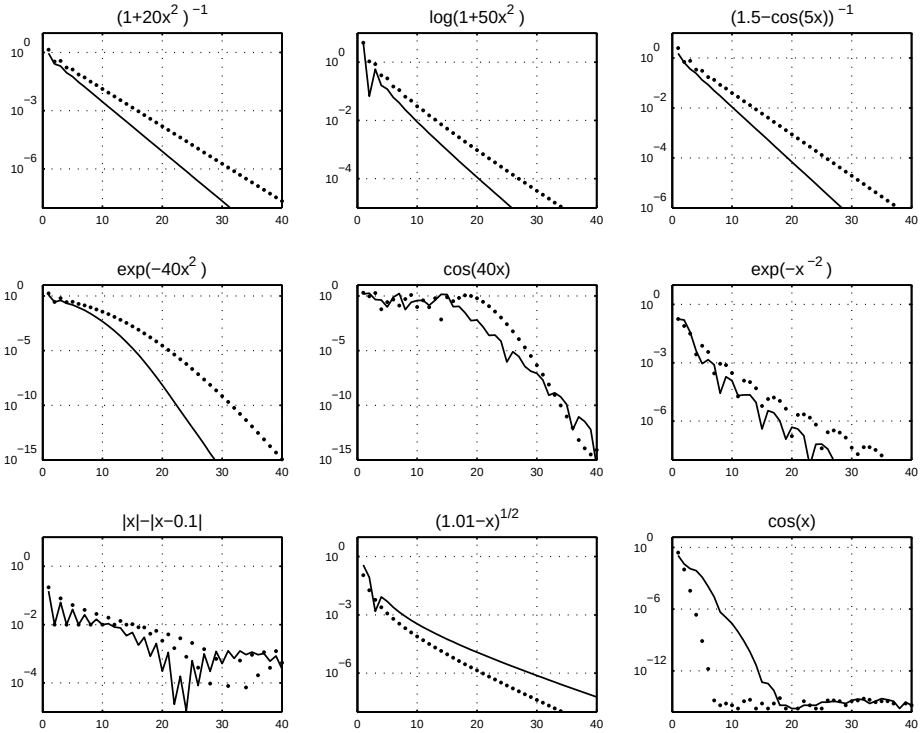

Figure 7: Comparison of Gauss quadrature (dots) against transplanted Gauss quadrature for the degree 9 polynomial (4.3) (solid), for the same nine integrands as in Figure 5. Again in many cases the transplanted formulas converge faster.

5 Related work

A number of ideas have been proposed over the years for combating the $\pi/2$ problem, both for quadrature and spectral methods, which might be classified as follows: (i) endpoint corrections, (ii) alternatives to polynomials, (iii) transplantation. Here is a brief summary of some of these developments.

The endpoint corrections idea starts from the observation that the trapezoid rule would achieve the ideal convergence rate if only the integrand were periodic. Accordingly, one might make some adjustments at the boundaries to achieve this effect, at least up to a prescribed order. The Euler–Maclaurin formula suggests one approach: one can add to the quadrature formula certain linear combinations of odd-order derivatives of the integrand at the endpoints, chosen to annihilate the error up to any prescribed power of the grid size. To get a quadrature rule based on function values only (i.e., without derivatives), one can then replace these terms by one-sided finite difference approximations of the appropriate orders. The resulting quadrature rules are known as *Gregory's formulas* [11, 30, 35], and they are effective up to medium orders of accuracy, at which point they encounter the difficulties caused by exponentially large coefficients of alternating signs. An improvement on Gregory formulas capable of achieving exponential convergence has been proposed by Alpert, building upon ideas of Rokhlin and Kapur [3, 31]. Alpert's method goes beyond the equispaced grid to include a small number of extra Gauss-like nodes near the endpoints, now with weights guaranteed to be positive. High-precision computations are required in advance to obtain the nodes and weights, but once they are known the method is highly effective.

By alternatives to polynomials we mean the explicit construction of orthogonal bases that are non-polynomial and have more uniform behavior over the interval of interest. An important set of functions in this connection are the *prolate spheroidal wave functions*, which were introduced by Slepian and coauthors in the 1960s [45]. These functions have excellent resolution properties, and more recent authors have shown their power for a variety of computational applications [9, 10, 13, 53]. In this literature, rather than derive theorems about convergence for functions analytic in specified domains as we are about to do, it is customary to quantify the matter of resolution by considering applications to band-limited functions.

Finally there is the transplantation idea, the basis of the present article. A notable contribution in this area is a forty-year-old theoretical paper by Bakhvalov, "On the optimal speed of integrating analytic functions" [4]. What is the optimal family of quadrature formulas, Bakhvalov asks, for the set of functions analytic and bounded by M in a given complex region Ω containing $[-1, 1]$? His first step is to transplant the problem by a conformal map g to an ellipse E_ρ. This is very close to what we have done, but with a difference. In the ellipse, the new quadrature problem has a weight g'. Since his aim is to investigate optimal formulas, Bakhvalov now considers the Gauss formulas associated with this weight, which he shows are in a sense optimal. By contrast we have used the unweighted Gauss formula, including g' instead as part of the integrand. We presume that this simpler procedure does not hurt the convergence rate much in practice, but we have not investigated this matter. Bakhvalov's paper is full of interesting ideas,

and it has led to subsequent developments in the theoretical quadrature literature by Petras and other authors [23, 28, 34, 40]. So far as we are aware, however, this collection of publications has not been concerned with the $\pi/2$ phenomenon, nor with particular choices of Ω, and does not propose actual quadrature formulas for use in practice.

A more practically oriented transplantation idea was introduced in the spectral methods literature by Kosloff and Tal-Ezer in 1993 [33]. Like the conformal maps proposed in the last section, the Kosloff–Tal-Ezer map is derived from the inverse sine function. Their transformation is

$$g(s) = \frac{\sin^{-1}(\alpha s)}{\sin^{-1}(\alpha)} \tag{5.1}$$

for a value of α slightly less than 1. Various methods for choosing α are considered both in their original paper and in various subsequent works by other authors [2, 15, 18, 29, 37].

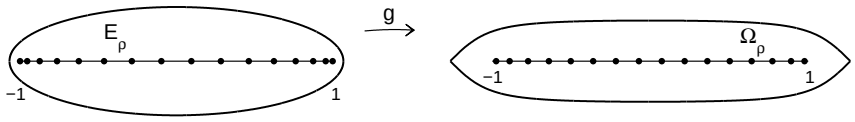

Figure 8: The Kosloff–Tal-Ezer map (5.1) for $\rho = 1.4$ and $\alpha = 2/(\rho + \rho^{-1}) \approx 0.9459$. For the given choice of ρ, this is the largest possible α for which g is analytic in E_ρ.

The Kosloff–Tal-Ezer map is quite different from those of §3 and §4 in original concept but rather similar in practice. These authors, and their successors, do not consider g as a conformal map, and they do not present theorems about geometric rates of convergence for analytic functions. Nevertheless the function (5.1) has the familiar effect of mapping E_ρ to a region with straighter sides, with the usual consequence that the nodes are distributed more evenly in the interior and clustered less near ± 1. To investigate a Kosloff–Tal-Ezer map in the framework established in this paper, we might begin by setting $\rho = 1.4$ and drawing a plot analogous to those of Figures 1, 2, and 6. The largest choice of α for which g will be analytic in E_ρ is $\alpha = 2/(\rho + \rho^{-1}) \approx 0.9459$. Figure 8 shows the result.[2]

The node spacings for the various transformations we have considered are shown (for $n = 24$) in Figure 9.

If we apply the Kosloff–Tal-Ezer map to the same nine test integrands as before, we get the curves shown in Figure 10. These results are good. Nevertheless, the strip-transplanted formula of Figure 5 does better for the first four functions, and the sausage-transplanted formula of Figure 7 does as well or better for the last five. There are parameters in all of these methods that might be tuned to enhance their performance, so one cannot draw fine judgments from these simple experiments. The proper lesson

[2]In [29] Hesthaven et al. consider a spectral method with $\alpha = \cos(1/2) \approx 0.88$, corresponding to $\rho \approx 1.69$. In most other spectral methods papers that make use of the Kosloff–Tal-Ezer mapping, α is chosen to increase toward 1 as n increases.

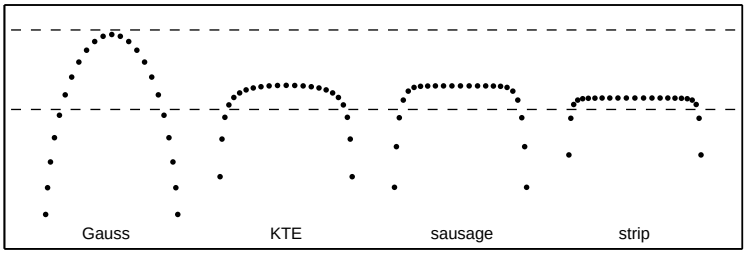

Figure 9: Comparison of node spacings with $n = 24$ for Gauss quadrature, the Kosloff–Tal-Ezer map (5.1) with $\rho = 1.4$ and $\alpha = 2/(\rho + \rho^{-1})$, the polynomial (4.3) of degree 9, and the strip map (3.2) with $\rho = 1.4$. Dots appear at horizontal positions $(x_j + x_{j+1})/2$ and vertical positions $(x_{j+1} - x_j)/2$. The dashed lines correspond to equally spaced points and the same times $\pi/2$.

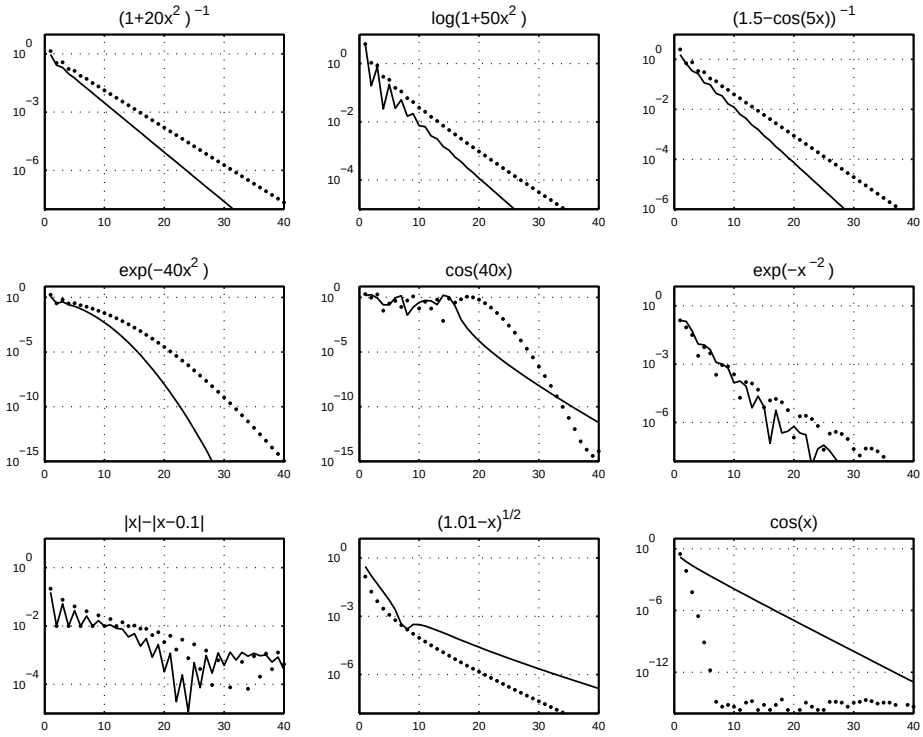

Figure 10: Another comparison of Gauss (dots) and transplanted Gauss (solid) quadrature for the integrands of Figures 5 and 7, now for the Kosloff–Tal-Ezer map (5.1) with $\rho = 1.4$ and $\alpha = 2/(\rho + \rho^{-1}) \approx 0.9459$.

is that all of these methods are capable of outperforming Gauss quadrature by 20–50% for many integrands. Let us now make this observation more precise.

6 Convergence theorems for analytic integrands

An advantage of the conformal mapping point of view is that it leads readily to convergence theorems for analytic integrands. The trick is to decide what analyticity assumptions and conformal maps g to consider, for the number of possibilities is unlimited. Rather than explore this terrain thoroughly we shall offer a few representative choices. Our class of integrands will be as follows. For any $\varepsilon > 0$:

$$\mathcal{A}(\varepsilon) = \text{set of functions analytic in the open } \varepsilon\text{-neighborhood of } [-1,1]. \tag{6.1}$$

Now the ellipse with foci ± 1 whose semiminor axis length is ε has parameter $\rho = \varepsilon + \sqrt{1+\varepsilon^2} = 1 + \varepsilon + O(\varepsilon^2)$. Since $\rho > 1 + \varepsilon$, any $f \in \mathcal{A}(\varepsilon)$ is bounded in the ellipse $E_{1+\varepsilon}$, and thus by Theorem 1, Gauss quadrature will achieve $I_n - I = O((1+\varepsilon)^{-2n})$ as $n \to \infty$ for any $f \in \mathcal{A}(\varepsilon)$. On the other hand since $\rho \sim 1 + \varepsilon$ as $\varepsilon \to 0$, it will do no better than this in general as $\varepsilon \to 0$. By contrast, the methods of the last three sections, with the parameters used there, converge at least 40%, 30%, and 30% faster, respectively.

Theorem 4 *Let the transplanted Gauss quadrature formula* (2.6) *be applied to a function $f \in \mathcal{A}(\varepsilon)$. The following statements pertain to the limit $n \to \infty$.*

For the strip map (3.2) *with $\rho = 1.4$, for any $\varepsilon \le 0.24$: $\tilde{I}_n - I = O((1+1.4\varepsilon)^{-2n})$.*

For the polynomial (4.3) *with $d = 9$, for any $\varepsilon \le 0.8$: $\tilde{I}_n - I = O((1+1.3\varepsilon)^{-2n})$.*

For the KTE map (5.1) *with $\rho = 1.4$, for any $\varepsilon \le 0.3$: $\tilde{I}_n - I = O((1+1.3\varepsilon)^{-2n})$.*

Proof Consider for example the first assertion, that the map (3.2) with $\rho = 1.4$ has convergence rate $O((1+1.4\varepsilon)^{-2n})$. By Theorem 1, this conclusion will be valid if for all $\varepsilon \le 0.24$, the function g is analytic in the elliptical region $E_{1+1.4\varepsilon}$ and maps the ellipse of parameter $1 + 1.4\varepsilon$ into the open ε-neighborhood of $[-1,1]$. We know that g is analytic throughout $E_{1.4}$, so the first condition holds since $1 + (1.4)(0.24) < 1.4$. The second condition can be verified numerically by plotting the image of the ellipse and the boundary of the ε-neighborhood for various ε and verifying that the first is inside the second; of course, we have chosen parameters in the theorem to make this true. ∎

The speedups of Theorem 4 are not particularly close to the limiting value of $\pi/2$ that can be achieved as $\varepsilon \to 0$. We now give another result that comes closer to this limit. This time we modify the Gauss quadrature estimate $O((1+\varepsilon)^{-2n})$ by improving the exponent rather than the factor multiplying ε.

Theorem 5 *Let the transplanted Gauss quadrature formula* (2.6) *be applied to a function $f \in \mathcal{A}(\varepsilon)$ for any $\varepsilon \le 0.05$. For the strip map* (3.2) *with $\rho = 1.1$, $\tilde{I}_n - I = O((1+\varepsilon)^{-3n})$ as $n \to \infty$.*

The proof is as before, combining Theorem 1 with a numerical verification for the particular map g. Similarly, it can be shown that one gets $\tilde{I}_n - I = O((1+\varepsilon)^{-2.7n})$ for $\varepsilon \le 0.1$ for the strip map (3.2) with $\rho = 1.4$, the higher-degree analogue of the polynomial (4.3) with $d = 17$, or the KTE map (5.1) with $\rho = 1.2$; and $\tilde{I}_n - I = O((1+\varepsilon)^{-2.5n})$ for $\varepsilon \le 0.3$ for the strip map (3.2) with $\rho = 1.5$, the polynomial (4.3) with $d = 9$, or the KTE map (5.1) with $\rho = 1.4$.

7 Clenshaw–Curtis variant

Among polynomial quadrature methods, Gauss quadrature is optimal from the point of view of degree of polynomials integrated exactly, namely $2n-1$ for the formula (2.2). It also has an elegant convergence theory for analytic integrands, as represented by Theorem 1 and the further theorems we have derived from it. Thus it is natural that in the experiments of this paper until now, we have considered Gauss quadrature and its transplanted alternatives.

Gauss quadrature has the disadvantage, however, that it takes $O(n^2)$ work and memory to compute Gauss nodes and weights by the standard algorithm of Golub and Welsch [27]. In some applications this is not an issue, because either n is small or the nodes and weights are precomputed. In others, it is troublesome indeed. Certainly one would rarely use a Gauss quadrature formula with thousands of points.

An easy alternative is Clenshaw–Curtis quadrature, which is readily implemented via the Fast Fourier Transform in $O(n \log n)$ operations [14, 26]; now there is no problem if n is 10^4 or 10^5 [6, 50]. All the conformal transplantation ideas discussed in this article can be applied to Clenshaw–Curtis as well as Gauss formulas, with comparable effect: a speedup for many integrands by a factor approaching $\pi/2$. A Clenshaw–Curtis code segment for $(n+1)$-point integration of f over $[-1,1]$ can be written like this [50]:

```
s = cos((0:n)'*pi/n);
[g,gprime] = strip(s);
fx = f(g).*gprime/(2*n);
h = real(fft(fx([1:n+1 n:-1:2])));
a = [h(1); h(2:n)+h(2*n:-1:n+2); h(n+1)];
w = 0*a'; w(1:2:end) = 2./(1-(0:2:n).^2);
In = w*a;
```

One's first expectation is that Clenshaw–Curtis convergence rates should generally be about half those of Gauss, both for the pure and the transplanted variants. For example, the n-point Clenshaw–Curtis formula exactly integrates polynomials only up to degree n, not $2n-1$, and similarly, a result like Theorem 1 holds with $O(\rho^{-2n})$ reduced to $O(\rho^{-n})$. Thus one might expect that a transplanted Clenshaw–Curtis formula should converge about $2 \times 2/\pi = 4/\pi$ times more slowly than untransplanted Gauss quadrature.

In actuality, however, Clenshaw–Curtis formulas are often about as accurate as Gauss, for the values of n of interest, despite what the standard theorems might lead

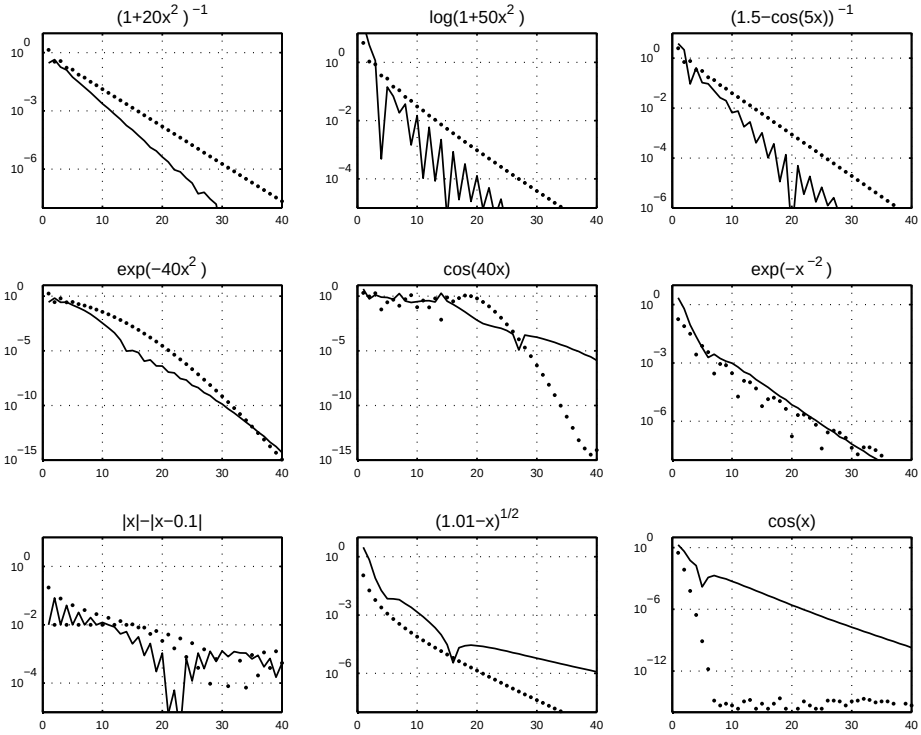

Figure 11: Another repetition of Figure 5, but with the solid curve corresponding now to strip-transplanted Clenshaw–Curtis rather than Gauss quadrature. The results are much the same as in Figure 5, the main exception being $\exp(-40x^2)$, where we now see a convergence rate that cuts in half at around $n = 14$. Evidently transplanted Clenshaw–Curtis quadrature, quite apart from its much greater speed of implementation, is often more accurate the Gauss quadrature as well.

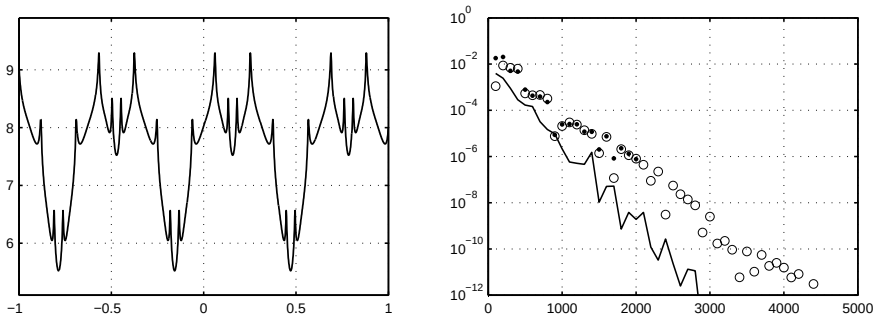

Figure 12: On the left, the function $f(x)$ adapted from [51]. On the right, convergence of Gauss (dots), Clenshaw–Curtis (circles), and strip-transplanted Clenshaw–Curtis formulas (solid) with $\rho = 1.1$ for this function. Data are plotted corresponding to values of n equal to multiples of 100 (up to $n = 2000$ for Gauss quadrature). There is no significant difference between the Gauss and Clenshaw–Curtis formulas, and the transplanted formula beats them both by about 50%, as one would expect for Gauss quadrature from Theorem 5.

one to expect. This effect was observed by O'Hara and Smith in the 1960s [39] and has recently been investigated further [21, 50, 52]. We find the same happy surprise with transplanted Clenshaw–Curtis quadrature. We shall make no attempt to add more to the theoretical discussion of this effect, but just present two computational illustrations. The first is Figure 11, another repetition of Figure 5 but now comparing pure Gauss quadrature against strip-transplanted Clenshaw–Curtis, again for $\rho = 1.4$. The latter does very well—about as well as transplanted Gauss. Indeed it is only for the function $\exp(-40x^2)$ where we have lost much in moving from transplanted Gauss to transplanted Clenshaw–Curtis: the convergence rate starts out as before but then cuts abruptly in half at an error level of about 10^{-5}. This kink in the Clenshaw–Curtis convergence curve for analytic functions is explained in [21, 50, 52].

Our second example is a complicated function $f(x)$ on $[-1, 1]$ considered in [51], defined by the initial conditions $f = \beta = \sin(10x)$ followed by 15 steps of the iteration $\beta = 3(1 - 2\beta^4)/4$, $f = f + \beta$. (In [51] the initial condition is $\sin(\pi x)$, but we change this to $\sin(10x)$ to break the periodicity.) Figure 12 illustrates f and the convergence of quadrature formulas to $I \approx 15.3198135546173$. Strip-transplanted Clenshaw–Curtis quadrature with $\rho = 1.1$ beats untransplanted Clenshaw–Curtis, which is more or less the same as Gauss. This function f is entire, but it is very ill-behaved outside a small region surrounding $[-1, 1]$, as illustrated in Figure 13. For example, the maximum value of $|f(z)|$ for $\operatorname{Im} z = 0.002$ is about 9.5, for $\operatorname{Im} z = 0.003$ it is about 3236, for $\operatorname{Im} z = 0.004$ it is about 10^{41}, and for $\operatorname{Im} z = 0.05$ it is about 10^{263}.

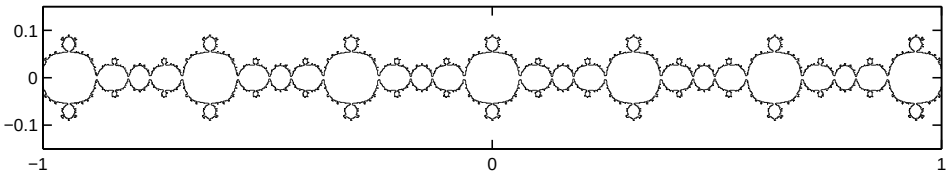

Figure 13: Although entire, the function f of Figure 12 is ill-behaved away from a strip of width about 0.003 surrounding $[-1,1]$. This plot shows the region around $[-1,1]$ in which $|f(x)| < 1000$. The boundary has a fractal structure 15 levels deep.

8 Discussion

The idea of transforming the integrand in a numerical quadrature rule is an old one. What is new in this paper has been to choose transformations based on explicit conformal maps and to thereby derive specific quadrature formulas that often converge faster than Gauss quadrature. Numerical experiments justifying this claim were presented in §3–§5 and §7, and theorems in §3 and §6.

All the methods we have discussed contain adjustable parameters, notably ρ for (3.2), the degree d for the maps of §4, and α for (5.1). Rather than try to optimize these values, we have taken somewhat arbitrary fixed choices such as $\rho = 1.4$ or 1.1 and $d = 9$ or 17, which are enough to deliver fairly robust quadrature improvements by 30%–50%. These figures could be increased closer to the 57% associated with the ratio $\pi/2$ by decreasing ρ and increasing d and α, perhaps in a fashion dependent on the number of grid points n, and in some applications, such adjustments may be worthwhile. There is a literature on how to choose α for the application of the Kosloff–Tal-Ezer map (5.1) to spectral methods [2, 15, 18, 29, 37]. Preliminary experiments show that the speedups we have described for quadrature appear equally for spectral methods, and we hope to give details in a later publication. For spectral methods there is the additional consideration that the diminished clustering near ± 1 permits larger time steps or faster iterative matrix solves, making the choice of effective parameters a more complicated matter.

To compute a single integral, or a small number of integrals, one would normally use an adaptive quadrature program, and we do not recommend Gauss or Clenshaw–Curtis formulas, or their transplanted improvements, for such applications. Indeed, even for the complicated integrand of Figure 12, transplanted Clenshaw–Curtis quadrature is less than ten times faster than MATLAB's general-purpose adaptive codes `quad` and `quadl`. Rather, the potential practical relevance of the methods investigated in this paper is to situations where large numbers of integrals are imbedded inside a bigger computation. We close with an artificial example of a multidimensional integral. Suppose we compute

$$\int_{-1}^{1}\int_{-1}^{1}\int_{-1}^{1}\int_{-1}^{1} \cos(100(w+x+y+z))\,dw\,dx\,dy\,dz = \left(\frac{\sin(100)}{50}\right)^4 \approx 1.05\times 10^{-8}$$

numerically by a quadrature formula applied in four dimensions, exploiting none of the symmetries or simple structure of this particular integrand. To get three digits of relative

accuracy, Gauss quadrature requires $63^4 = 15{,}752{,}961$ points, whereas strip-transplanted Gauss quadrature with $\rho = 1.4$ needs $52^4 = 7{,}311{,}616$ points.

Acknowledgments

We are grateful for helpful suggestions to Gregory Beylkin, Adam Chandler, Toby Driscoll, Christian Lubich, Ricardo Pachón, and André Weideman.

Appendix. Computation of the strip transformation in extreme cases, and a MATLAB code

Figure 3 shows how the conformal map g of (3.2) from the ρ-ellipse E_ρ to the infinite strip Ω_ρ can be constructed in three steps: ellipse→periodic strip→disk→infinite strip, with the middle step involving a Jacobi elliptic function. All this is mathematically straightforward, but when ρ is smaller than about 1.1, it is numerically troublesome. The problem is that the right end of the periodic strip gets mapped in the disk domain to the interval $[1, m^{-1/4}]$, and this interval shrinks exponentially as ρ decreases to 1 (similarly at the left end). For example, $\rho = 1.4, 1.2, 1.1$ correspond to $m^{-1/4} \approx 1.0026, 1.0000053, 1.000000000023$, and for $\rho = 1.05$ one calculates $m^{-1/4} = 1$ on a computer to machine precision. This "crowding phenomenon" is a familiar challenge in numerical conformal mapping, making it impossible to compute g accurately unless the computation is reformulated [20].

It would be possible to consider systematically the development of an algorithm to evaluate g to as close to machine precision as possible. Rather than attempt this, we propose a method that works very well for our quadrature application and is much simpler. When ρ is small, the two ends of the rectangle→strip map of Figure 3 are exponentially decoupled from one another. In fact, for ρ less than about 1.2, the map near one end of the rectangle is indistinguishable in 16-digit arithmetic from what it would be if the rectangle were a semi-infinite strip. By following this line of reasoning, after quite of bit of algebra, one is led to consider the function g defined by $u = \sin^{-1} s$, $\tau = \pi/\log\rho$, and

$$g(s) = C\left[\log(1+e^{-\tau(\pi/2+u)}) - \log(1+e^{-\tau(\pi/2-u)}) + \left(\frac{1}{2} + \frac{1}{e^{\tau\pi}+1}\right)\tau u\right], \quad (8.1)$$

where the constant C is fixed so that $g(\pm 1) = \pm 1$. To 16-digit precision, for $\rho < 1.2$, this function is the same as the strip map (3.2); and it is numerically reliable down to about $\rho = 1.02$, which is closer to 1 than one would ever need to go in practice. For $s \in (-1, 1)$ the derivative is

$$g'(s) = \frac{-\tau C}{\sqrt{1-s^2}}\left[\frac{1}{e^{\tau(\pi/2+u)}+1} + \frac{1}{e^{\tau(\pi/2-u)}+1} - \left(\frac{1}{2} + \frac{1}{e^{\tau\pi}+1}\right)\right], \quad (8.2)$$

and at the endpoints we have

$$g'(\pm 1) = \frac{C\tau^2}{4} \tanh^2(\frac{\tau\pi}{2}). \tag{8.3}$$

Notice how much more elementary (8.1)–(8.2) are than (3.1)–(3.4). In principle g is not analytic in the ellipse, having branch points at $s = \pm 1$. The singularities are so weak, however, that for $\rho < 1.2$ they are undetectable in 16-digit arithmetic.

Although the map (8.1) was derived as an approximation to the ideal (3.2) for small values of ρ, it is surprisingly effective even for larger values of ρ. If (3.2) is replaced by (8.1) in the experiments of Figure 5, for example, it makes no difference.

The following terse code combines all the elements we have discussed, implementing the Clenshaw–Curtis quadrature formula for the modified strip transformation (8.1). Since such a code will be especially useful for large n, the listing gives a value of ρ close to 1. If this code is applied to the function of Figure 12 with $n = 1800$, it gets the right answer to 15 digits in about 0.01 seconds on a 2006 workstation. (With $n = 10^6$ it gets the same answer in 5 seconds.) Untransformed Gauss quadrature with $n = 1800$ achieves 11 digits of accuracy and takes far longer.

```
function I = CCstrip(f,n)                              % transplanted C-C quad.
rho = 1.1; t = pi/log(rho);                            % rho (adjustable) and tau
d = .5+1/(exp(t*pi)+1); p2 = pi/2;                     % convenient abbreviations
up = pi*(0:n)/n; u = up-p2; um = p2-u;                 % u and shifts by +-pi/2
C = 1/(log(1+exp(-t*pi))-log(2)+p2*t*d);
g = C*(log(1+exp(-t*up))-log(1+exp(-t*um))+u*t*d); % map g
gp = 1./(exp(t*up)+1)+1./(exp(t*um)+1)-d;
gp(2:n) = -t*C*gp(2:n)./cos(u(2:n));
gp([1 n+1]) = C*(t*tanh(p2*t)/2)^2;                    % derivative g'
fx = f(g).*gp/(2*n);                                   % transplanted integrand
h = real(fft(fx([1:n+1 n:-1:2])));                     % Chebyshev coefficients
a = [h(1) h(2:n)+h(2*n:-1:n+2) h(n+1)];
w = 0*a; w(1:2:n+1) = 2./(1-(0:2:n).^2);               % Clenshaw-Curtis weights
I = w*a';                                              % the result
```

References

[1] M. Abramowitz and I. A. Stegun, *Handbook of Mathematical Functions,* Dover, 1972 (originally published in 1964).

[2] M. R. Abril-Raymundo and B. García-Archilla, Approximation properties of a mapped Chebyshev method, *Appl. Numer. Math.* 32 (2000), 119–136.

[3] B. K. Alpert, Hybrid Gauss-trapezoidal quadrature rules, *SIAM J. Sci. Comp.* 20 (1999), 1551–1584.

[4] N. S. Bakhvalov, On the optimal speed of integrating analytic functions, *USSR Comput. Math. Math. Phys.* 7 (1967), 63–75.

[5] W. Barrett, On the convergence of Cotes' quadrature formulae, J. Lond. Math. Soc. 39 (1964), 296–302.

[6] Z. Battles and L. N. Trefethen, An extension of MATLAB to continuous functions and operators, *SIAM J. Sci. Comp.* 25 (2004), 1743–1770.

[7] A. Bayliss and E. Turkel, Mappings and accuracy for Chebyshev pseudo-spectral approximations, *J. Comp. Phys.* 101 (1992), 349–359.

[8] S. Bernstein, Quelques remarques sur l'interpolation, *Math. Ann.* 79 (1919), 1–12.

[9] G. Beylkin and K. Sandberg, Wave propagation using bases for bandlimited functions, *Wave Motion* 41 (2005), 263–291.

[10] J. P. Boyd, Prolate spheroidal wavefunctions as an alternative to Chebyshev and Legendre polynomials for spectral element and pseudospectral algorithms, *J. Comp. Phys.* 199 (2004), 688–716.

[11] H. Brass, *Quadraturverfahren*, Vandenhoeck and Ruprecht, Göttingen, 1977.

[12] C. Canuto, M. Y. Hussaini, A. Quarteroni and T. A. Zang, *Spectral Methods: Fundamentals in Single Domains*, Springer, 2006.

[13] Q.-Y. Chen, D. Gottlieb and J. S. Hesthaven, Spectral methods based on prolate spheroidal wave functions for hyperbolic PDEs, *SIAM J. Numer. Anal.* 43 (2005), 1912–1933.

[14] C. W. Clenshaw and A. R. Curtis, A method for numerical integration on an automatic computer, *Numer. Math.* 2 (1960), 197–205.

[15] B. Costa, W. S. Don and A. Simas, Exponential convergence of mapped Chebyshev methods, manuscript, 2007.

[16] P. J. Davis and P. Rabinowitz, *Methods of Numerical Integration,* 2nd ed., Academic Press, New York, 1984.

[17] Z. Ditzian and V. Totik, *Moduli of Smoothness*, Springer-Verlag, New York, 1987.

[18] W.-S. Don and A. Solomonoff, Accuracy enhancement for higher derivatives using Chebyshev collocation and a mapping technique, *SIAM J. Sci. Comput.* 18 (1997), 1040–1055.

[19] T. A. Driscoll, Algorithm 843: Improvements to the MATLAB toolbox for Schwarz–Christoffel mapping, *ACM Trans. Math. Softw.* 31 (2005), 239–251.

[20] T. A. Driscoll and L. N. Trefethen, *Schwarz–Christoffel Mapping,* Cambridge U. Press, 2002.

[21] D. Elliott, B. M. Johnston and P. R. Johnston, Clenshaw–Curtis and Gauss-Legendre quadrature for certain boundary element integrals, manuscript, 2006.

[22] H. Engels, *Numerical Quadrature and Cubature,* Academic Press, London, 1980.

[23] P. Favati, G. Lotti and F. Romani, Bounds on the error of Fejér and Clenshaw–Curtis type quadrature for analytic functions, *Appl. Math. Lett.* 6 (1993), 3–8.

[24] H. E. Fettis, Note on the computation of Jacobi's nome and its inverse, *Computing* 4 (1969), 202–206.

[25] W. Gautschi, A survey of Gauss–Christoffel quadrature formulae, in P. L. Butzer and F. Fehér, eds., *E. B. Christoffel,* Birkhäuser, Basel, 1981, pp. 72–147.

[26] W. M. Gentleman. Implementing Clenshaw–Curtis quadrature I and II, *Comm. ACM* 15 (1972), 337–346, 353.

[27] G. H. Golub and J. H. Welsch, Calculation of Gauss quadrature rules, *Math. Comp.* 23 (1969), 221–230.

[28] M. Götz, Optimal quadrature for analytic functions, *J. Comp. Appl. Math.* 137 (2001), 123–133.

[29] J. S. Hesthaven, P. G. Dinesen and J. P. Lynov, Spectral collocation time-domain modelling of diffractive optical elements, *J. Comp. Phys.* 155 (1999), 287–306.

[30] F. B. Hildebrand, *Introduction to Numerical Analysis,* 2nd ed., Dover, 1987 (originally published in 1974).

[31] S. Kapur and V. Rokhlin, Higher-order corrected trapezoidal quadrature rules for singular functions, *SIAM J. Numer. Anal.* 34 (1997), 1331–1356.

[32] T. Koch and J. Liesen, The conformal 'bratwurst' maps and associated Faber polynomials, *Numer. Math.* 86 (2000), 173–191.

[33] D. Kosloff and H. Tal-Ezer, A modified Chebyshev pseudospectral method with an $O(N^{-1})$ time step restriction, *J. Comp. Phys.* 104 (1993), 457–469.

[34] M. A. Kowalski, A. G. Werschulz and H. Woźniakowski, Is Gauss quadrature optimal for analytic functions?, *Numer. Math.* 47 (1985), 89–98.

[35] E. Martensen, Optimale Fehlerschranken füer die Quadraturformel von Gregory, *Z. Angew. Math. Mech.* 44 (1964), 159–168.

[36] V. I. Krylov, *Approximate Calculation of Integrals,* Dover, 2005 (originally published in 1962).

[37] J. L. Mead and R. A. Renaut, Accuracy, resolution, and stability properties of a modified Chebyshev method, *SIAM J. Sci. Comput.* 24 (2002), 143–160.

[38] M. Mori and M. Sugihara, The double-exponential transformation in numerical analysis, *J. Comp. Appl. Math.* 127 (2001), 287–296.

[39] H. O'Hara and F. J. Smith, Error estimation in the Clenshaw–Curtis quadrature formula, *Computer J.* 11 (1968), 213–219.

[40] K. Petras, Gaussian versus optimal integration of analytic functions, *Constr. Approx.* 14 (1998), 231–245.

[41] G. Pólya, Über die Konvergenz von Quadraturverfahren, *Math. Z.* 37 (1933), 264–286.

[42] P. Rabinowitz, Rough and ready error estimates in Gaussian integration of analytic functions, *Comm. ACM* 12 (1969), 268–270.

[43] T. W. Sag and G. Szekeres, Numerical evaluation of high-dimensional integrals, *Math. Comp.* 18 (1964), 245–253.

[44] C. Schwartz, Numerical integration of analytic functions, *J. Comp. Phys.* 4 (1969), 19–29.

[45] D. Slepian and H. O. Pollak, Prolate spheroidal wave functions, Fourier analysis and uncertainty. I, *Bell System Tech. J.* 40 (1961), 43–63.

[46] F. Stenger, *Numerical Methods Based on Sinc and Analytic Functions,* Springer, 1993.

[47] H. Takahasi and M. Mori, Double exponential formulas for numerical integration, *Publications RIMS, Kyoto U.* 9 (1974), 721–741.

[48] T. W. Tee and L. N. Trefethen, A rational spectral collocation method with adaptively transformed Chebyshev grid points, *SIAM J. Sci. Comp.* 28 (2006), 1798–1811.

[49] L. N. Trefethen, *Spectral Methods in MATLAB*, SIAM, Philadelphia, 2000.

[50] L. N. Trefethen, Is Gauss quadrature better than Clenshaw–Curtis?, *SIAM Review,* to appear.

[51] L. N. Trefethen, Computing numerically with functions instead of numbers, *Math. in Computer Sci.*, submitted.

[52] J. A. C. Weideman and L. N. Trefethen, The kink phenomenon in Fejér and Clenshaw–Curtis quadrature, *Numer. Math.*, submitted.

[53] H. Xiao, V. Rokhlin, and N. Yarvin, Prolate spheroidal wavefunctions, quadrature and interpolation, *Inverse Problems* 17 (2001), 805–838.